



# Large area porous gold films deposited by evaporation-induced colloidal crystal growth

Renyun Zhang \*, Magnus Hummelgård, Håkan Olin \*

Department of Natural Sciences, Engineering and Mathematics, Mid Sweden University, SE 851 70 Sundsvall, Sweden

## ARTICLE INFO

### Article history:

Received 14 May 2009

Accepted 6 August 2009

Available online 12 August 2009

### Keywords:

Porous gold

Thin film

Self-assembly

Evaporation-induced colloid crystal growth

Conductivity

## ABSTRACT

Films that are nanostructured in two- or three-dimensions, such as porous ones, are made by several methods including templated growth and self-assembly. Here, we report on a new method that is based on evaporation-induced growth of nanoparticle gold films on a water surface. The film growth was done in a similar way to the well-known evaporation-induced colloidal crystal growth method, but in contrast, we did not directly deposit the film on a solid substrate. The films were instead created on top of a water surface. After the growth process, the films were deposited directly on substrates by a simple pick-up procedure. The deposited porous gold films were uniform with a thickness of 100 nm and had a sheet resistance of 100  $\Omega$ /sq. There are several advantages with our method, including simplicity of the protocol, large film area, flexibility in the choice of substrate to be coated, and the ability for multilayer coatings. The latter points to opportunities for fabrication of multilayer 3D porous structure, which may have wide applications in sensors and electrochemical determinations.

© 2009 Elsevier Inc. All rights reserved.

## 1. Introduction

Nanostructured materials with high surface area have attracted much attention due to their applications in many areas such as sensors [1], catalysis [2], optics [3] 2D and 3D porous metal films have recently been interested since they permit easy fabrication of devices or electrodes [4]. Porous gold nanomaterials are the most well studied of the metal materials. To fabricate porous gold films or networks, several methods have been used, such as dealloying [5–10], templating [11–13], electrochemical deposition [4], and wet chemical methods [14,15]. These methods rely on various protocols; the dealloying methods depend on the reactivity of two components, which permit selective dissolution [5]. The templating methods need several steps, including template deposition, target materials cover, and template removal [9]. The templating method may, for example, be started with a film of Au/Ag mixture, and then porous gold film is obtained by removing the Ag nanoparticles [16]. Electrochemical deposition contains an oxidation–reduction procedure that starts from a bulk gold electrode in HCl solution [4]. Wet chemical methods for synthesizing gold nanowire networks are performed by adjusting the amount of citrate [14].

All these methods are performed in several steps and for most of them; the porous gold films are fabricated by removing compo-

nents from the gold containing films. However, there are simpler protocols, where the gold nanoparticles themselves self-assemble into porous structures. For example, there are reports on 2D films obtained by self-assembly of gold nanoparticles in the presence of surfactants [17] or alkyl dithiol/alkanethiol links [18,19]. Another recent example is the self-assembled growth method of gold nanowhiskers films, using a diffusion-limited aggregation method [20]. One important method along this self-assembly route is evaporation driven convective assembly that have been investigated during the last decade [21–24]. The observed films using evaporation driven convective assembly are well ordered 3D film, since both face centered-cubic (fcc) and hexagonally close-packed (hcp) structures could form good films. For this evaporation type of assembly both theory [25] and review [26] papers are published.

The reported gold films are all deposited on substrates unless there are surfactant participates [17], however a free standing gold film on top of water without any surfactant molecules may be desired, since such a film could be easily transferred to many substrates.

Here, we report on a new simple method that is similar to evaporation driven convective assembly, but the film is floating at the liquid surface without any surfactant. These single layer porous films were uniform in thickness. An advantage of such a floating film is that it can be deposited on any suitable substrate, simply by placing the substrate beneath the film and subtract it. The method should thus allow a number of applications, such as electronics, surface coating and so on.

\* Corresponding authors.

E-mail addresses: renyun.zhang@miun.se (R. Zhang), hakan.olin@miun.se (H. Olin).

## 2. Experimental

### 2.1. Synthesis of gold nanoparticles

A 1.0 ml 1.0wt% HAuCl<sub>4</sub> (Sigma) solution was added into 99.0 ml doubly distilled water and heated to boil while stirring, then, 4.0 ml 1.0wt% sodium citrate (Sigma) was added [27]. The solution was kept boiling for 5–10 min, until the solution turned to a red wine color.

### 2.2. Self-assembly of gold film

The synthesized colloid gold solution was stored in a 100 ml beaker with a diameter of 6 mm. The 100 ml beaker was covered by a 1000 ml beaker in order to avoid dust from the air. The solution was kept in the lab with the temperature of  $21 \pm 1$  °C and a humidity of  $30 \pm 2$ %.

### 2.3. TEM characterization

For TEM characterization, a 400 M gold grid without carbon film was put under the gold film, and then deposited by retracting the grid from the solution. The grid was dried at room temperature for 20 min. TEM imaging was done using a JEOL 2000FX transmission electron microscope at 160 kV accelerate voltage.

### 2.4. SEM characterization

SEM characterizations were performed on an EVO50 (Zeiss). The samples for SEM were either the same as used for TEM, or prepared by coating the gold film on a SiO<sub>2</sub> wafer. The latter samples were also used for AFM and *I/V* measurements.

### 2.5. AFM characterization

AFM imaging was carried out on a dimension AFM (Digital Instruments) using tapping mode. The sample for AFM imaging was the same as that used for SEM characterization, which was a gold film deposited on SiO<sub>2</sub> wafer.

### 2.6. Current/voltage (*I/V*) measurements

*I/V* measurements were performed on a micromanipulator 1800 wafer probe station (Micromanipulator), using two stainless wires as source and drain electrodes.

### 2.7. Surface tension measurements

Surface tension tests were performed in another parallel sample of the colloid gold solution, which were at the same condition as the one that we used to collect films.

## 3. Results and discussion

In our experiments, gold nanoparticles were synthesized by the reaction of HAuCl<sub>4</sub> and sodium citrate [27]. A TEM image of the synthesized gold nanoparticles was given in [Supplementary material](#) as Fig. S1. The obtained solution was kept at ambient condition for 4–7 days in a beaker. After that, a thin film with golden color appeared at the water surface and with an area of up to several square centimeters (see photo in [Supplementary material](#), Fig. S2). One could deposit the film on any substrate by hand or using a method similar Langmuir–Blodgett technique [26]. In our experiment we took out the film using oxidized Si wafers or TEM grids (400 M, gold grids, without carbon film).

Fig. 1 shows scanning electron microscope images of the obtained film at low and high magnification. Some defects on the film can be found in Fig. 1A, and that might be due to the thermal disturbance of the water flow or some mechanical vibration in the room. Yet at higher magnification, as shown in Fig. 1B, the structure is quite uniform, indicating a monolayer of gold nanowires. In the SEM images (Fig. S3 in [Supplementary material](#)) it is also apparent that the resulting film is relatively uniform in height. For comparison, SEM images of the gold film after 3 and 5 days evaporation are shown in [Supplementary material](#) as Fig. S4.

Fig. 2 shows a transmission electron microscope image of the gold film. The diameters of the wires were in the range of 40–100 nm, and the distance between adjacent gold nanowires were in the range of 80–300 nm. Furthermore, at the surface of the nanowires, some smaller particles could be found. These gold nanoparticles were the original synthesized nanoparticles with a size of  $9 \pm 1$  nm. These absorbed nanoparticles indicate that the growth of the nanowires were due to aggregation of particles that sintered together and formed larger nanowires. Formation of nanowires by sintering of nanoparticles has also been observed using the surfactant method [17], which indicate that the sintering of gold nanoparticles is due to the increase of surface pressure. In contrast, as reported previously, the evaporation-induced convective assembly is able to fabricate nanoparticle layers but the nanoparticles do not coalescence into larger particles [25,26].

An atomic force microscope (AFM) image of the obtained film on an oxidized Si surface is shown in [supplementary material](#), which indicated the average thickness of the film was about 100 nm ([Supplementary material Fig. S5](#)). In the AFM image larger spherical aggregates are visible that resulted from the sintering of the original 9 nm nanoparticles. This is consistent with the TEM image in Fig. 2 where the spherical aggregates are also visible,

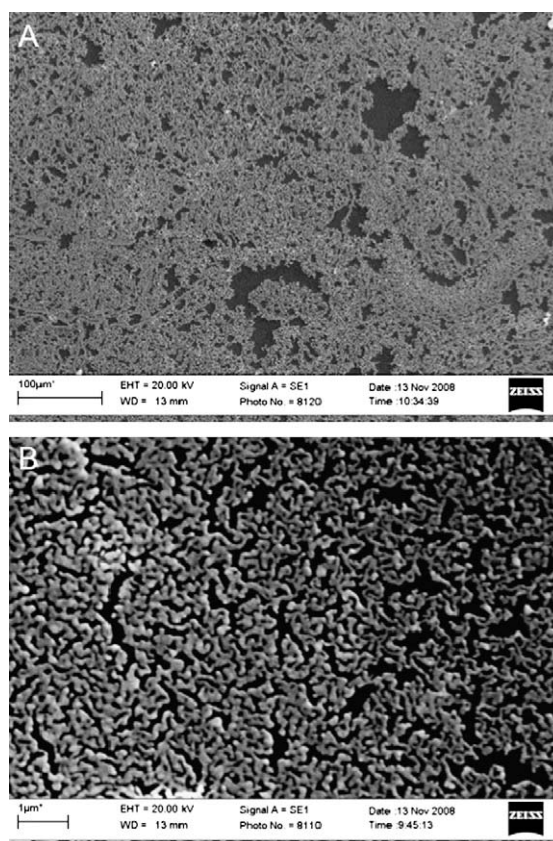
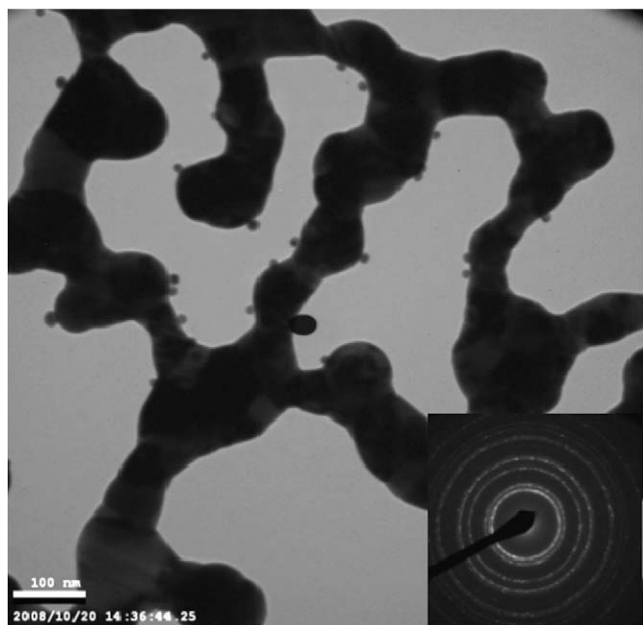


Fig. 1. SEM images of single layer gold film at low (A) and high (B) magnification.



**Fig. 2.** TEM image of the gold nanowire film. The insert image shows the diffraction pattern of the gold nanowires. (The black dot in the center of the images is an imaging artifact).

but in addition the TEM image also show how they are actually sintered together in a net.

Electrical characterization was done by measuring current–voltage ( $I/V$ ) curves using two electrical probes at different places on a 100 nm thick film, with the same distance between the electrodes. The  $I/V$  curves, obtained from four different places, were all linear (see [Supplementary material](#), Fig. S6). The average resistance from 10  $I/V$  curves was  $24.7 \Omega$  with a STD of 0.9 with a probe separation distance of 1 mm. The low spread shows that the conductance of the gold film was quite uniform at different places. We can make a rough estimate of the sheet resistance ( $R_s$ ) using a correction [28] of  $\text{Pi}/\ln 2 = 4.53$  to the resistance and assume zero resistance at shorter distances, giving an  $R_s$  of about  $100 \Omega/\text{sq}$ . This could be compared with a perfect 100 nm thick gold film with bulk resistivity that should have a sheet resistance of  $0.2 \Omega/\text{sq}$  (from  $R_s = \text{resistivity}/\text{thickness}$  and bulk resistivity of  $22 \text{ n}\Omega/\text{m}$ ), or with porous gold film fabricated on a porous aluminum template that have a  $R_s$  of  $4\text{--}15 \Omega/\text{sq}$  for a film thickness of about 100 nm [29].

Since the gold films are floating on top of the solution, it should be easy to fabricate double layers or multilayers of gold films by two or more steps. This layer-by-layer fabrication may serve as a procedure to construct 3D porous gold films, which may have wide applications in sensors and catalysis due to the unique properties of gold nanowires. We did such multilayer deposition and Fig. 3 shows a SEM image of a double layers gold film (a SEM image of three layers gold film was shown in [Supplementary material](#) as Fig. S7). These 3D porous structures have large surface area, and might provide a nice platform for molecules absorption or for increasing detection signals in sensors.

Fig. 4 shows schematic processes of the evaporation-induced gold film growth. When water starts to evaporate from the colloidal gold solution the gold nanoparticles assembled on the wall of the beaker, which is a well-investigated procedure [25,26]. For the assembly and crystal growth of gold wires with gold nanoparticles, mechanisms were reported elsewhere [30,31]. When the water continued to evaporate, the concentration of gold nanoparticle increased, and this induced a growth of the gold film on the solution surface and formed the single gold nanowire layer. When the

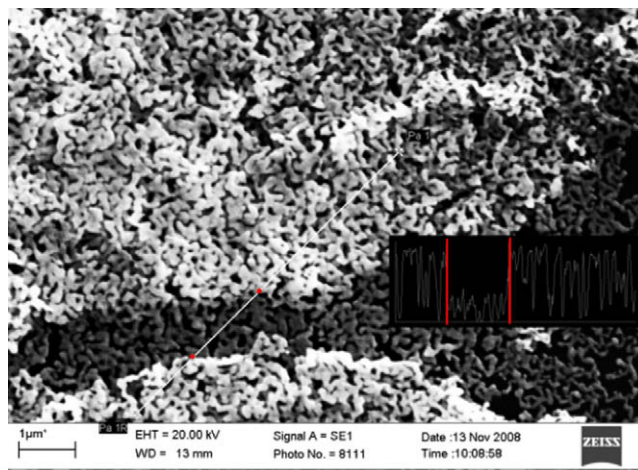


**Fig. 3.** SEM image of double layer porous gold film. The insert shows the contrast of the film on the sample line.

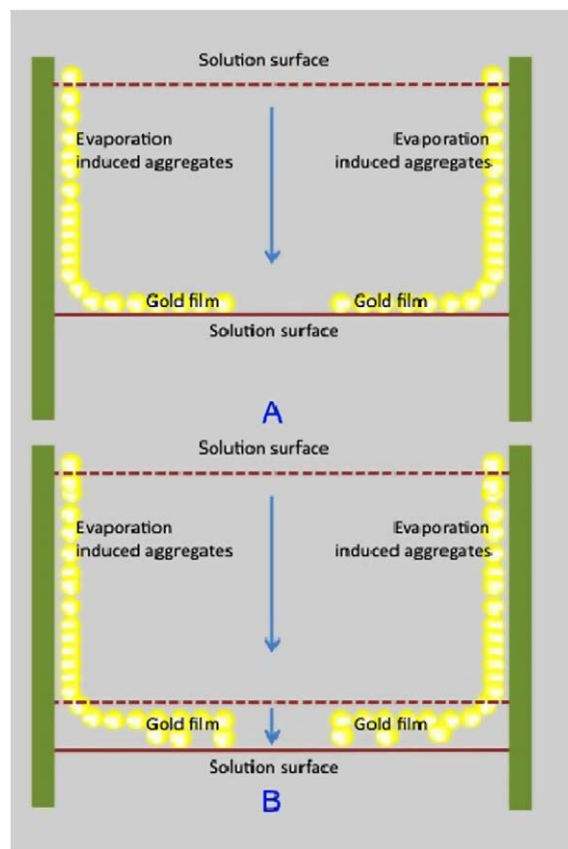


**Fig. 4.** Schematic processes of the growth of different porous gold films. (A) During the first 4–7 days; (B) after one additional week for (A).

nanoparticles sinter with each other and forming larger structures the hydrophobicity will increase, helping the gold film to float on the water surface. The golden color of the floating film that we observed, indicate that the film had the surface properties of bulk gold, which is hydrophobic.

We also checked the surface tension as a function of time. When the density of the solution increased the surface tension also increased slightly from  $71.8 \text{ mN/m}$  to  $73.0 \text{ mN/m}$  (see [Supplementary material](#), Fig. S8). This increase in surface tension might also contribute to making the gold film float.



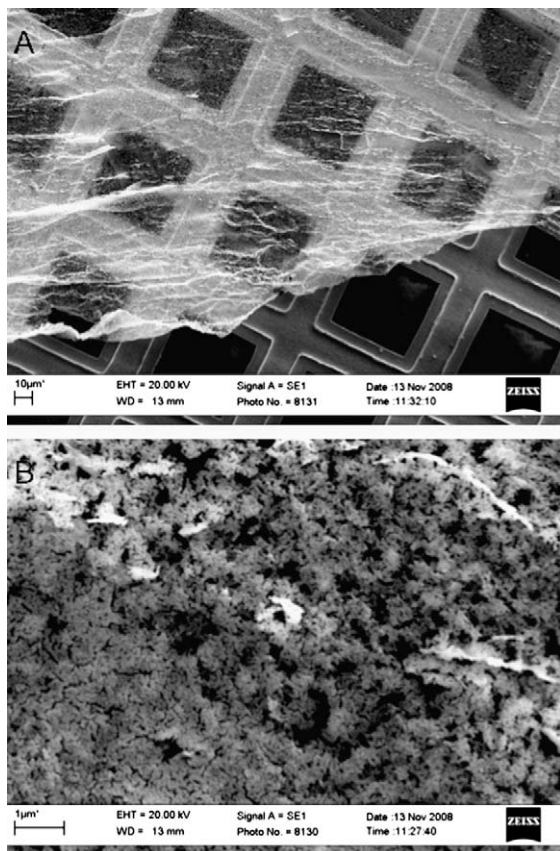


**Fig. 5.** SEM images of porous gold films after 14 days of growth. (A) and (B) show the low and high magnification image, respectively. The highly porous structure is visible in (B).

After a week of evaporation, the gold film was more or less covering the surface and when the process was continued for yet another week the film started to grow in thickness instead of area. The film grew in 3D with a more porous structure (as shown in Fig. 5). Since the gold nanoparticle concentration was very high at this stage, and the surface of the solution was occupied by the previous grown film, the gold nanoparticles started to aggregate on the already assembled gold film. The growth mechanism is however different in this case. Instead of the ordering and sintering on the surface as in the first single layer growth, the nanoparticles stick to the assembled film from below and this process leads to a more disordered, porous structure. This 3D growth is shown schematically in Fig. 4B.

#### 4. Conclusions

In summary, we studied evaporation-induced growth of porous gold films. Our results demonstrate that the evaporation-induced colloidal crystal growth could be grown at the surface of a liquid, not only at some solid interfaces as reported previously. The aggregated gold nanoparticles first formed a single layer on the water surface. Furthermore, the gold nanoparticles could form 3D porous structures grown on the single layer gold film, when the evaporation time was extended and the gold nanoparticle concentration

increased. This floating film could be deposited on a surface and characterization showed a 100 nm single layer porous film of uniform thickness with a sheet resistance of about 100  $\Omega$ /sq. Multilayers were formed by repeating the deposition procedure, pointing to opportunities for fabrication of multilayer 3D porous structure, which may have wide applications such as for sensors. In addition, since gold is a good electrode material, this large area porous gold film with good conductance may be used for electrochemical determinations.

#### Acknowledgment

We thank Sundsvall Community for financial support.

#### Appendix A. Supplementary material

Supplementary data associated with this article can be found, in the online version, at [doi:10.1016/j.jcis.2009.08.006](https://doi.org/10.1016/j.jcis.2009.08.006).

#### References

- [1] M. Lahav, A.N. Shipway, I. Willner, M.B. Nielsen, J.F. Stoddart, *J. Electroanal. Chem.* 482 (2000) 217–221.
- [2] M.C. Daniel, D. Astruc, *Chem. Rev.* 104 (2004) 293–346.
- [3] Y. Lu, Y.D. Yin, Z.Y. Li, Y.N. Xia, *Nano Lett.* 2 (2002) 785–788.
- [4] Y.P. Deng, W. Huang, X. Chen, Z.L. Li, *Electrochem. Commun.* 10 (2008) 810–813.
- [5] F.L. Jia, C.F. Yu, Z.H. Ai, L.Z. Zhang, *Chem. Mater.* 19 (2007) 3648–3653.
- [6] L.H. Qian, X.Q. Yan, T. Fujita, A. Inoue, M.W. Chen, *Appl. Phys. Lett.* 90 (2007) 153120.
- [7] J.T. Zhang, P.P. Liu, H.Y. Ma, Y. Ding, *J. Phys. Chem. C* 111 (2007) 10382–10388.
- [8] S.O. Kuchetev, J.R. Hayes, J. Biener, T. Huser, C.E. Talley, A.V. Hamza, *Appl. Phys. Lett.* 89 (2006) 053102.
- [9] T. Fujita, L.H. Qian, K. Inoue, J. Erlebacher, M.W. Chen, *Appl. Phys. Lett.* 92 (2008) 251902.
- [10] J. Snyder, K. Livi, J. Erlebacher, *J. Electrochem. Soc.* 155 (2008) C464–C473.
- [11] W. Gao, X.H. Xia, J.J. Xu, H.Y. Chen, *J. Phys. Chem. C* 111 (2007) 12213–12219.
- [12] P.N. Bartlett, J.J. Baumberg, P.R. Birkin, M.A. Ghanem, M.C. Netti, *Chem. Mater.* 14 (2002) 2199–2208.
- [13] F.C. Meldrum, R. Seshadri, *Chem. Commun.* 1 (2000) 29–30.
- [14] L.H. Pei, K. Mori, M. Adachi, *Langmuir* 20 (2004) 7837–7843.
- [15] T. Wang, X.G. Hu, J.L. Wang, S.J. Dong, *Talanta* 75 (2008) 455–460.
- [16] Y.G. Lu, Q.F. Wang, J.Q. Sun, J.C. Shen, *Langmuir* 21 (2005) 5179–5184.
- [17] T. Hassenkam, K. Nørgaard, L. Iversen, C.J. Kiely, M. Brust, T. Bjørnholm, *Adv. Mater.* 14 (2002) 1126–1130.
- [18] G.R. Wang, L.Y. Wang, Q. Rendeng, J.G. Wang, J. Luo, C.J. Zhong, *J. Mater. Chem.* 17 (2007) 457–462.
- [19] L. Han, M.M. Maye, F.L. Leibowitz, N.K. Ly, C.J. Zhong, *J. Mater. Chem.* 11 (2001) 1258–1264.
- [20] T. Qiu, X.L. Wu, G.G. Siu, P.K. Chu, *Appl. Phys. Lett.* 87 (2005) 223115.
- [21] K.P. Velikov, C.G. Christova, R.P.A. Dullens, A. van Blaaderen, *Science* 296 (2002) 106–109.
- [22] S. Wong, V. Kitaev, G.A. Ozin, *J. Am. Chem. Soc.* 125 (2003) 15589–15598.
- [23] P. Jiang, J.F. Bertone, K.S. Hwang, V.L. Colvin, *Chem. Mater.* 11 (1999) 2132–2140.
- [24] B.G. Prevo, O.D. Velev, *Langmuir* 20 (2004) 2099–2107.
- [25] D.D. Brewer, J. Allen, M.R. Miller, J.M. de Santos, S. Kumar, D.J. Norris, M. Tsapatsis, L.E. Scriven, *Langmuir* 23 (2008) 13683.
- [26] D.J. Norris, E.G. Arlinghaus, L.L. Meng, R. Heiny, L.E. Scriven, *Adv. Mater.* 16 (2004) 1393–1399.
- [27] L.A. Gearheart, H.J. Ploehn, C.J. Murphy, *J. Phys. Chem. B* 105 (2001) 12609–12615.
- [28] Y. Huang, H. Qiu, H. Qian, F.Q. Wang, L.Q. Pan, P. Wu, Y. Tian, X.L. Huang, *Thin Solid Film* 472 (2005) 302.
- [29] S.A. Collette, M.A. Sutton, P. Miney, A.P. Reynolds, X.D. Li, P.E. Colavita, W.A. Scrivens, Y. Luo, T. Sudarshan, P. Muzykov, M.L. Myrick, *Nanotechnology* 15 (2004) 1812–1817.
- [30] S. Biggs, P. Mulvaney, C.F. Zukoski, F. Grieser, *J. Am. Chem. Soc.* 116 (1994) 9150–9157.
- [31] B.K. Pong, H.I. Elim, J.X. Chong, W. Ji, B.L. Trout, J.Y. Lee, *J. Phys. Chem. C* 111 (2007) 6281–6287.